THE JOURNAL OF PHYSICAL CHEMISTRY Letters

Letter

pubs.acs.org/JPCL

Polymer Single Crystal As Magnetically Recoverable Support for Nanocatalysts

Bin Dong, David L. Miller, and Christopher Y. Li*

Department of Materials Science and Engineering, Drexel University, Philadelphia, Pennsylvania 19104, United States

Supporting Information

ABSTRACT: In this Letter, we report, for the first time, using polymer single crystal as magnetically recoverable support for nanoparticle catalysts. This catalyst system is composed of polymer single crystal, platinum nanoparticles, and iron oxide nanoparticles, which act as support, catalysts, and magnetic responsive materials, respectively. Platinum nanoparticles and iron oxide nanoparticles were bonded onto thiol groups and hydroxyl groups on a tailor-designed polymer single-crystal surface. Because of its quasi 2D nature, polymer single crystal possesses high surface area to volume ratio (2.5×10^8 m^{-1}), which is ~40 times higher than its nanosphere counterpart of the same volume. This high surface to volume ratio facilitates the high loading of both nanoparticles, which ensures efficient catalytic reaction and reliable nanoparticle recycling. Synergetic interactions between platinum and iron oxide nanoparticles also led to further improvement in catalytic activity.

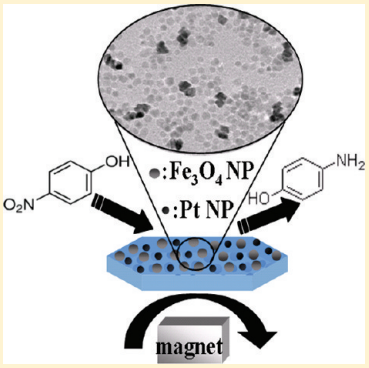

SECTION: Glasses, Colloids, Polymers, and Soft Matter

Metallic nanoparticle catalysts have attracted increasing attention in recent years because of their high catalytic activity.[1,2] This high activity is partially originated from the high surface to volume ratio due to the small nanoparticle sizes. The major challenge of employing metallic nanoparticle catalyst in various application fields is two-fold. First, it is difficult to prevent nanoparticles from forming agglomerates, which decreases the nanoparticle surface area; hence the catalytic capability drops. Second, recycling nanoparticles is not a trivial task because they are small in size.[3] One solution to overcome these problems is to use catalyst support.[4] The utilization of catalyst support not only helps to disperse and stabilize nanoparticles but also facilitates separation and reuse of catalysts from the reaction system. Commonly used catalyst supports for metallic nanoparticles can be classified into two categories: inorganic and organic supports.[5] As compared with inorganic support (e.g., carbon,[6] silica,[7] metal oxide[8]), organic support has the advantages such as versatility (they can be easily functionalized) and chemical inertness (no interference with the catalyst).[9] Commonly used organic supports are micrometer- or submicrometer-sized beads made of PMMA,[10] PS,[11] and so on, which is easy to recycle. However, to realize the maximum catalyst loading and activity, it is desirable to use support with a higher specific surface area. Although it is possible to realize this by reducing the size of organic support to sub-100 nm scale, the recycling of support itself is problematic when using the conventional separation method such as centrifugation. A possible solution to this contradiction is to only reduce the size of organic support in one dimension and fabricate quasi-2D catalyst support, which has significantly improved surface area to volume ratio. The 2D nature of the support also ensures high loading of multiple functional nanoparticles for both catalysis and recycling.[12]

One example of such quasi-2D materials is polymer single crystals (PSCs), which typically adopt a lamellar morphology with a thickness of a few nanometers.[13,14] By controlling the number of nuclei using self-seeding technique,[15−17] PSCs with uniform sizes ranging from a few tens of nanometers to hundreds of micrometers can be readily grown in solution. When end-functionalized polymer is utilized as the source material, under carefully controlled crystallization conditions, end functional groups can be excluded onto the surface of PSC, resulting in PSCs with exposed functional groups.[18] Because end-functionalized polymers can be readily synthesized, different functional groups such as thiol, hydroxyl, and silane can be introduced onto the crystal surface, which in turn can be used to immobilize functional materials, for example, gold nanoparticle (AuNP),[17−20] iron oxide nanoparticle (Fe_3O_4NP),[21] and quantum dots.[22] In addition, the thinness of the PSCs also leads to a high specific surface area, which is critical to catalyst support applications.

In this Letter, we report, for the first time, the utilization of PSCs as magnetically recyclable support for nanoparticle catalysts. As a proof of concept, we selected platinum nanoparticles (PtNPs) as the catalytic component and Fe_3O_4NPs as the magnetic responsive materials. To attach both nanoparticles, the support is composed of PSCs with two different types of surface groups, that is, thiol (−SH) and

Received: April 10, 2012
Accepted: May 1, 2012
Published: May 1, 2012

dx.doi.org/10.1021/jz300434c | J. Phys. Chem. Lett. 2012, 3, 1346−1350

hydroxyl (−OH) (Scheme 1), because −SH can attach to a variety of surfaces, such as platinum, gold, silver, iron oxide,[21]

Scheme 1. Schematic Illustration of the Fabrication Process of Magnetically Responsive Polymer Single Crystal for Nanocatalyst Support

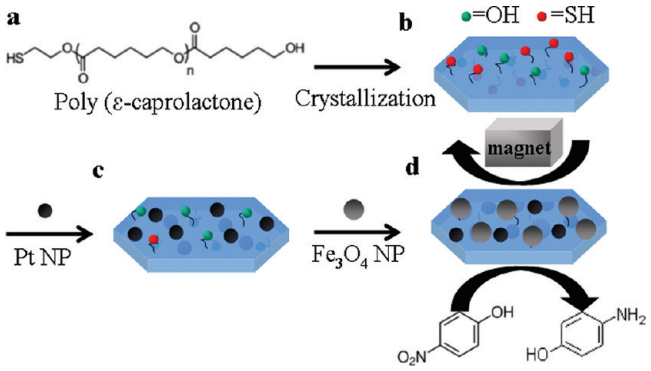

and so on, whereas −OH can bond to iron oxide surface.[23] Because of the thinness of PSCs, high loading of both PtNPs and Fe_3O_4NP has achieved, which maximize both the catalytic activity and separation/recycling efficiency. An interesting additional advantage the current system brings is that due to the high loading of two different types of nanoparticles, the contact areas between these two nanoparticles generate synergetic effect, which further increases the catalytic activity.

Scheme 1 outlines the process we utilized to synthesize PSCs/nanoparticle ensembles. α-hydroxy-ω-thiol terminated polycaprolactone (PCL) (HO-PCL-SH in abbreviation) with a molecular weight of 13.2 K g/mol was synthesized according to literature.[24] Uniformly sized HO-PCL-SH single crystal was obtained using the self-seeding method.[25] In brief, HO-PCL-SH was first dissolved in 1-butanol at 60 °C for 10 min. The solution was stored at 5 °C for 2 h and subsequently brought to the seeding temperature (T_s) of 46 °C for 10 min to obtain the crystal seeds. The seed-containing polymer solution was then allowed to crystallize at the crystallization temperature (T_c) of 22 °C for 24 h to obtain HO-PCL-SH single crystals. The as-fabricated HO-PCL-SH single crystal has a hexagon shape (Figure 1a inset). It is 13 μm long and 5 μm wide. The thickness was determined by using atomic force microscopy (AFM) to be ∼8 nm, as shown in Figure 1a,b. Because PSCs have a relatively constant thickness that is determined by the crystallization temperature,[26] their surface area to volume ratio can be estimated to be $\sim 2/t$, where t is the thickness of the PSC (neglecting the side surface of the PSC because it is much smaller than the top/bottom surface). Note that this value is independent of the single-crystal lateral size. The surface area to volume ratio in the present case therefore can be calculated to be $\sim 2.5 \times 10^8$ m^{-1}, which is equivalent to that of a nanosphere with a 12 nm radius! In contrast, a sphere with similar volume (∼0.45 μm^3) has a surface area to volume ratio of only about 6.3×10^6 m^{-1}, ∼40 times less than what PSC can offer. This implies that thin polymer lamellar crystal could be an excellent candidate for catalyst support. Surface functionalization is critical to immobilize the targeted particle on the PSC surface. In the present case, after crystallization, the end functional groups (OH and SH) were exposed onto the single-crystal surface (Scheme 1b), rendering the surface functionality of the PSC. HO-PCL-SH single crystal was then mixed with a PtNP solution. After saturated adsorption, PtNP was immobilized on single-crystal surface through thiol-platinum bond (Scheme 1c). Iron oxide nanoparticles were then introduced to bond to OH groups (and free SH groups, if any) on the PSC surface (Scheme 1d).

Figure 1c shows the TEM image of the HO-PCL-SH single crystal surface after incubating in the PtNP solution (zoom out view of the single crystal is shown in Figure 1c inset), which

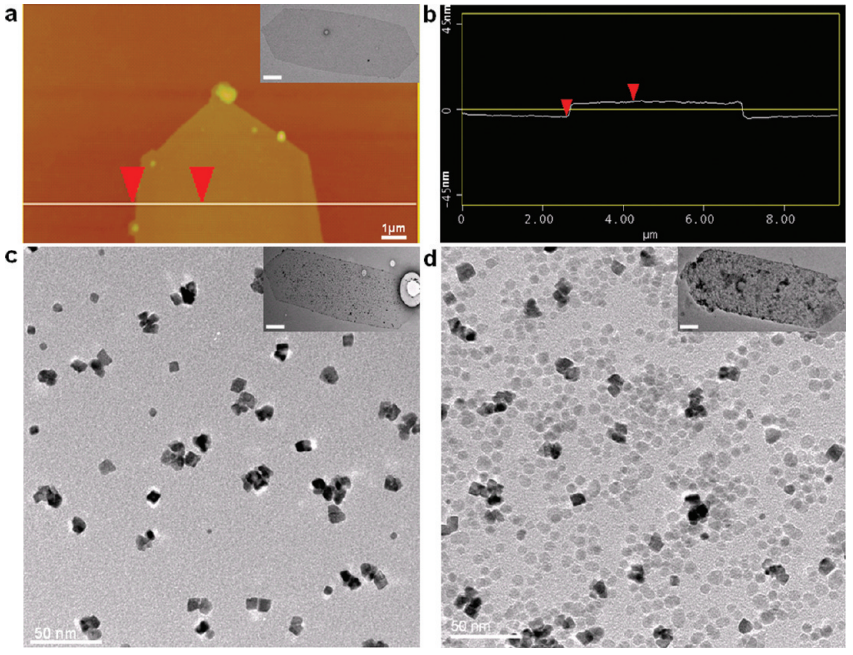

Figure 1. (a) Height mode AFM image of HO-PCL-SH single crystal. (b) Cross section analysis showing the thickness of HO-PCL-SH single crystal is around 8 nm. (c,d) TEM images of 7 nm PtNP-coated and 7 nm PtNP/10 nm Fe_3O_4NP-decorated HO-PCL-SH single crystals, respectively. Insets of panels a, c, and d show the zoom-out view of the corresponding single crystals. Scale bar for all insets: 1 μm.

dx.doi.org/10.1021/jz300434c | J. Phys. Chem. Lett. 2012, 3, 1346−1350

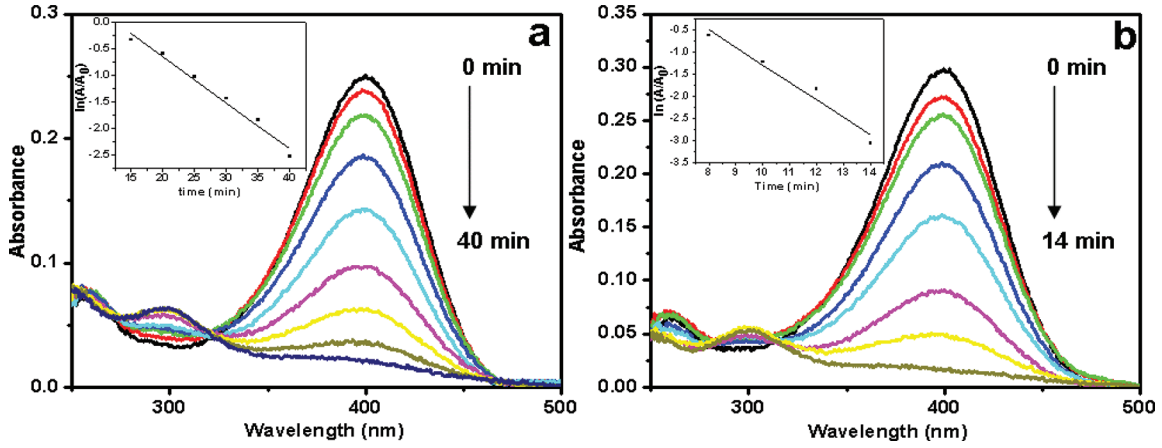

Figure 2. UV spectra of nitrophenol reduction reaction for (a) PSC/PtNP during 40 min reaction with 5 min interval and (b) PSC/PtNP/Fe_3O_4NP during 14 min reaction with 2 min interval. Inset: linear relationship of $\ln(A/A_0)$ as a function of time.

indicates that PtNPs have been immobilized on HO-PCL-SH single crystal surface through thiol-platinum bond. The areal number density of PtNPs is ~440/μm^2, and the catalyst loading can be estimated to be ~20% by weight. Figure 1d shows the TEM image of a HO-PCL-SH single crystal after adsorbing two types of nanoparticles. Because of their difference in atomic number, the dark PtNPs and light colored Fe_3O_4NPs can be easily distinguished under TEM (Figure 1d). The number density of PtNPs after Fe_3O_4NP attachment remains unchanged, indicating that there is no PtNP detachment during the second nanoparticle adsorption process. In Figure 1d, there are more Fe_3O_4NPs than PtNPs. Given that the areal densities of −SH and −OH on the surface of PCL single crystals are identical and that PtNP can bond only to −SH groups, whereas Fe_3O_4NP can bond to both −SH and −OH groups,[21] it can be concluded that after the first PtNP saturated adsorption, there are still free −SH groups that did not bond to any PtNPs and subsequently bonded to Fe_3O_4NP during the second Fe_3O_4NP adsorption process.

Reduction of 4-nitrophenol to 4-aminophenol by sodium borohydride has been frequently used as a model reaction to check the catalytic activity of metallic nanoparticles because it has no side reaction and can be easily monitored by UV−vis spectroscopy. This reaction is believed to involve the following processes: sodium borohydride adsorbed onto nanoparticle surface to form metal hydride and then 4-nitrophenol adsorbed onto nanoparticle surface; finally, 4-nitrophenol is reduced and desorbed to create a free space for the reaction to continue.[27] Figure 2a shows successive UV−vis spectra of 4-nitrophenol reduction solution in the presence of HO-PCL-SH single-crystal-supported 7 nm PtNP (PSC/PtNP in abbreviation). The spectra were taken at 5 min interval. 4-Nitrophenolate anion, which forms after the addition of sodium borohydride, shows a strong absorption peak at 400 nm. As time lapses, the peak intensity decreases. At the same time, the peak at 300 nm, which corresponds to 4-aminophenol, increases. The appearance of the isosbestic point at 314 nm indicates that there is no side reaction. The changes in absorption peaks are also reflected in solution color changes. The yellow color originated from 4-nitrophenol gradually faded as the reaction proceeds. This reaction is first order in 4-nitrophenol concentration after a delay time,[28] which is the time required for the reactants to diffuse onto nanoparticle surface. The apparent rate constant was calculated in this case to be ~0.08 min^{-1}, as shown in Figure 2a inset. Figure 2b shows the UV−vis spectra of 4-nitrophenol reaction when using HO-PCL-SH single-crystal-supported PtNP and Fe_3O_4NP (PSC/PtNP/Fe_3O_4NP in short) as catalyst. The amount of PtNP added to the reaction solution was kept the same as that of PSC/PtNP without Fe_3O_4NPs. The reduction completed in 40 min for Figure 2a and in 14 min for Figure 2b. The apparent rate constant increased from 0.08 min^{-1} in Figure 2a to ~0.4 min^{-1} in Figure 2b. Because the HO-PCL-SH supported Fe_3O_4NP has only negligible catalytic activity, as evidenced in Figure S1 of the Supporting Information, the five-fold increase in apparent rate constant must be derived from the interaction between PtNP and Fe_3O_4NP. Sun et al. have previously shown that the dumbbell Pt/Fe_3O_4NP exhibited enhanced activity when used in catalytic reaction.[29] As can be seen from Figure 1d, almost all PtNPs are surrounded by Fe_3O_4NP on the PSC surface. The contact areas between them should generate similar synergetic effect, that is, electrons transfer from Fe_3O_4 to Pt, which leads to the formation of electron-rich Pt, rendering the PtNP inside PtNP/Fe_3O_4NP ensemble catalytically more active.[29] Consequently, the catalytic reaction, which takes place on the PtNP surface, proceeds faster. Fe_3O_4NP has two functions in current study: effective magnetic separation and catalytic activity enhancement. Therefore, high Fe_3O_4NP/PtNP ratio is desired, which is the case in Figure 1d, where both Fe_3O_4NP and PtNP have reached their saturated adsorption under the present experimental condition. The current method does not allow for the effective control of Fe_3O_4NP adsorption exclusively to the proximity of the PtNPs. As a result, lowering the Fe_3O_4NP/PtNP ratio leads to isolated PtNPs that are not surrounded by any Fe_3O_4NPs, resulting in a lower reaction rate. We have further compared the present rate constant of PSC/PtNP with that of similar systems,[9] which was fabricated by first synthesizing nanoparticles and then immobilizing them onto polymer support. The catalytic activity is characterized under the same sodium borohydride (30 mM) and 4-nitrophenol concentration (0.015 mM). The rate constant in our current system is estimated to be 0.01 s^{-1} m^{-2} L when normalized by nanoparticle surface area and 0.08 s^{-1} g^{-1} L when normalized by the total weight of catalyst and support, which is 2.5 and 26 times higher than the reported literature value,[9] respectively.

Although it is difficult to separate small Fe_3O_4NP from solution because of their weak magnetic response, introducing Fe_3O_4NP assemblies consisting of many of them may

dx.doi.org/10.1021/jz300434c | J. Phys. Chem. Lett. 2012, 3, 1346−1350

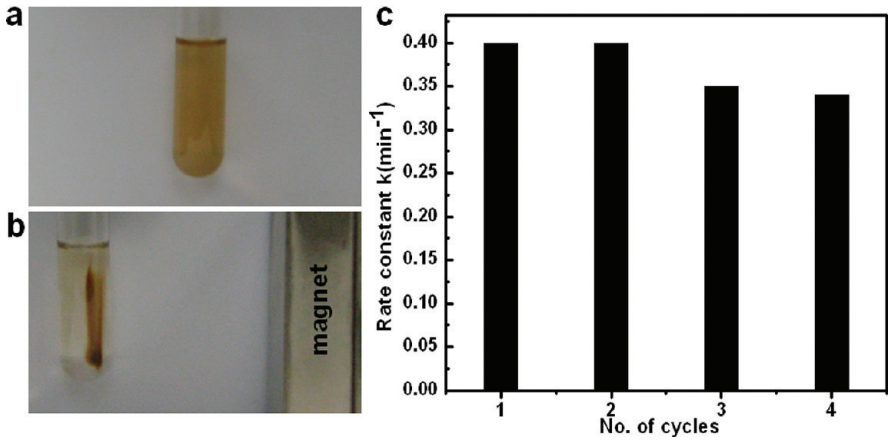

Figure 3. Photo image of PSC/PtNP/Fe_3O_4NP dispersed in 4-nitrophenol aqueous solution before (a) and after (b) applying a magnet. (c) Changes in apparent rate constant as the cycling continue.

significantly improve the separation efficiency. As evidenced in Figure 1d, the surface of HO-PCL-SH single crystal can be heavily loaded with a dense layer of Fe_3O_4NPs. Such high loading of Fe_3O_4NP ensures the efficient nanoparticle recycling. Figure 3a,b shows a photo image of the solution containing PSC/PtNP/Fe_3O_4NP before and after applying a magnet. All PSC/PtNP/Fe_3O_4NP can be quickly separated out to the side wall of the test tube under magnetic field, demonstrating that it is recyclable. We further evaluate the catalytic behavior of our system after magnetic recycling. The reaction catalyzed by PSC/PtNP/Fe_3O_4NP was first monitored by UV−vis spectrometer until its completion. Then, the catalyst was separated out using a magnet, rinsed, and redispersed in deionized water for the next cycle of catalysis. As shown in Figure 3c, the nanocatalyst can be magnetically recycled and reused four times with only slight changes in apparent rate constant.

In conclusion, we demonstrate, for the first time, the utilization of PSC as a magnetic recyclable support for nanocatalysts. This was achieved by controlled crystallization of HO-PCL-SH into single crystals with −OH and −SH groups on the crystal surface. These functional groups are capable of capturing both nanocatalyst (PtNP) and magnetic responsive materials (Fe_3O_4NP). Because of the synergetic interaction between PtNP and Fe_3O_4NP, this unique PSC/PtNP/Fe_3O_4NP ternary hybrid material showed enhanced catalytic activity as compared with the PSC/PtNP counterpart. Because of the high specific surface area of PSCs, the loading of both nanoparticles is high, which ensures not only the high catalytic activity when used in chemical reaction but also convenient separation from reaction solution under external magnetic field.

■ ASSOCIATED CONTENT

Ⓢ Supporting Information

Experimental details and control experiment. This material is available free of charge via the Internet at http://pubs.acs.org.

■ AUTHOR INFORMATION

Corresponding Author

*E-mail: chrisli@drexel.edu.

Notes

The authors declare no competing financial interest.

■ ACKNOWLEDGMENTS

This work was supported by the NSF (DMR-0804838 and CMMI-1100166). TEM experiments were carried out at the Drexel's Centralized Research Facility. We would like to thank Dr. Timothy Wade for assisting AFM experiments.

■ REFERENCES

(1) Thomas, J. M.; Johnson, B. F. G.; Raja, R.; Sankar, G.; Midgley, P. A. High-Performance Nanocatalysts for Single-Step Hydrogenations. *Acc. Chem. Res.* **2003**, *36*, 20−30.

(2) Burda, C.; Chen, X. B.; Narayanan, R.; El-Sayed, M. A. Chemistry and Properties of Nanocrystals of Different Shapes. *Chem. Rev.* **2005**, *105*, 1025−1102.

(3) Moshfegh, A. Z. Nanoparticle Catalysts. *J. Phys. D: Appl. Phys.* **2009**, *42*, 232001.

(4) Corma, A.; Garcia, H. Supported Gold Nanoparticles as Catalysts for Organic Reactions. *Chem. Soc. Rev.* **2008**, *37*, 2096−2126.

(5) Roucoux, A.; Schulz, J.; Patin, H. Reduced Transition Metal Colloids: A Novel Family of Reusable Catalysts. *Chem. Rev.* **2002**, *102*, 3757−3778.

(6) Kamat, P. V. Graphene-Based Nanoarchitectures. Anchoring Semiconductor and Metal Nanoparticles on a Two-Dimensional Carbon Support. *J. Phys. Chem. Lett.* **2010**, *1*, 520−527.

(7) Li, H. F.; Lu, J. A.; Zheng, Z. L.; Cao, R. An Efficient and Reusable Silica/Dendrimer Supported Platinum Catalyst for Electron Transfer Reactions. *J. Colloid Interface Sci.* **2011**, *353*, 149−155.

(8) Reetz, M. T.; Quaiser, S. A.; Breinbauer, R.; Tesche, B. A New Strategy in Heterogeneous Catalysis: The Design of Cortex Catalysts. *Angew. Chem., Int. Ed.* **1995**, *34*, 2728−2730.

(9) Mahmoud, M. A.; Snyder, B.; El-Sayed, M. A. Polystyrene Microspheres: Inactive Supporting Material for Recycling and Recovering Colloidal Nanocatalysts in Solution. *J. Phys. Chem. Lett.* **2010**, *1*, 28−31.

(10) Youk, J. H. Preparation of Gold Nanoparticles on Poly(methyl methacrylate) Nanospheres with Surface-Grafted Poly(allylamine). *Polymer* **2003**, *44*, 5053−5056.

(11) Ou, J. L.; Chang, C. P.; Sung, Y.; Ou, K. L.; Tseng, C. C.; Ling, H. W.; Ger, M. D. Uniform Polystyrene Microspheres Decorated with Noble Metal Nanoparticles Formed without Using Extra Reducing Aagent. *Colloids Surf., A* **2007**, *305*, 36−41.

(12) Polshettiwar, V.; Luque, R.; Fihri, A.; Zhu, H. B.; Bouhrara, M.; Bassett, J. M. Magnetically Recoverable Nanocatalysts. *Chem. Rev.* **2011**, *111*, 3036−3075.

(13) Li, B.; Li, L. Y.; Wang, B. B.; Li, C. Y. Alternating Patterns on Single-Walled Carbon Nanotubes. *Nat. Nanotechnol.* **2009**, *4*, 358−362.

(14) Li, C. Y. Polymer Single Crystal Meets Nanoparticles. *J. Polym. Sci., Part B: Polym. Phys.* **2009**, *47*, 2436−2440.

(15) Blundell, D. J.; Keller, A. A New Self-Nucleation Phenomenon and Its Application to the Growing of Polymer Crystals from Solution. *Polym. Lett.* **1966**, *4*, 481−486.
(16) Cai, W.; Li, C. Y.; Li, L.; Lotz, B.; Keating, M.; Marks, D. Sub-micro Tube/scroll Polymer Single Crystal from Nylon 6,6. *Adv. Mater.* **2004**, *16*, 600−605.
(17) Li, B.; Wang, B. B.; Ferrier, R. C. M.; Li, C. Y. Programmable Nanoparticle Assembly via Polymer Single Crystals. *Macromolecules* **2009**, *42*, 9394−9399.
(18) Li, B.; Li, C. Y. Immobilizing Au Nanoparticles with Polymer Single Ccrystals, Patterning and Asymmetric Functionalization. *J. Am. Chem. Soc.* **2007**, *129*, 12−13.
(19) Wang, B. B.; Li, B.; Zhao, B.; Li, C. Y. Amphiphilic Janus Gold Nanoparticles via Combining "Solid-State Grafting-to" and "Grafting-from" Methods. *J. Am. Chem. Soc.* **2008**, *130*, 11594−11595.
(20) Li, B.; Ni, C.; Li, C. Y. Poly(ethylene oxide) Single Crystals as Templates for Au Nanoparticle Patterning and Asymmetrical Functionalization. *Macromolecules* **2008**, *41*, 149−155.
(21) Dong, B.; Li, B.; Li, C. Y. Janus Nanoparticle Dimers and Chains via Polymer Single Crystals. *J. Mater. Chem.* **2011**, *21*, 13155−13158.
(22) Wang, B. B.; Li, B.; Ferrier, R. C. M.; Li, C. Y. Polymer Single Crystal Templated Janus Nanoparticles. *Macromol. Rapid Commmun.* **2010**, *31*, 169−175.
(23) Love, J. C.; Estroff, L. A.; Kriebel, J. K.; Nuzzo, R. G.; Whitesides, G. M. Self-Assembled Monolayers of Thiolates on Metals as a Form of Nanotechnology. *Chem. Rev.* **2005**, *105*, 1103−1169.
(24) Hedfors, C.; Ostmark, E.; Malmstrom, E.; Hult, K.; Martinelle, M. Thiol End-Functionalization of Poly(ε-caprolactone), Catalyzed by Candida Antarctica Lipase B. *Macromolecules* **2005**, *38*, 647−649.
(25) Girolamo, M.; Keller, A.; Stejny, J. Single Crystals of Linear Polyesters. *Makromol. Chem.* **1975**, *176*, 1489−1502.
(26) Wunderlich, B. *Macromolecular Physics*; Academic Press: New York, 1976; Vol. *II*.
(27) Wunder, S.; Polzer, F.; Lu, Y.; Mei, Y.; Ballauff, M. Kinetic Analysis of Catalytic Reduction of 4-Nitrophenol by Metallic Nanoparticles Immobilized in Spherical Polyelectrolyte Brushes. *J. Phys. Chem. C* **2010**, *114*, 8814−8820.
(28) Mei, Y.; Sharma, G.; Lu, Y.; Ballauff, M.; Drechsler, M.; Irrgang, T.; Kempe, R. High Catalytic Activity of Platinum Nanoparticles Immobilized on Spherical Polyelectrolyte Brushes. *Langmuir* **2005**, *21*, 12229−12234.
(29) Wang, C.; Daimon, H.; Sun, S. H. Dumbbell-like Pt-Fe_3O_4 Nanoparticles and Their Enhanced Catalysis for Oxygen Reduction Reaction. *Nano Lett.* **2009**, *9*, 1493−1496.